Influence of white matter inhomogeneous anisotropy on EEG forward computing

R. Bashar[1], Y. Li[1] and P. Wen[2]

[1]*Department of Mathematics and Computing, Centre for Systems Biology, University of Southern Queensland, Toowoomba, Australia*
[2]*Faculty of Engineering and Surveying, Centre for Systems Biology, University of Southern Queensland, Toowoomba, Australia*

Abstract

In this paper, we model the human head using the Volume and Wang's constraint methods, and study the inhomogeneous anisotropic conductivity for white matter (WM) using finite element method (FEM). To represent the WM accurately, the conductivity ratio approximation (CRA) and statistical conductivity approximation (SCA) techniques are applied to assign inhomogeneous anisotropic conductivity. This model is evaluated and compared with a homogeneous isotropic model and a homogeneous anisotropic model. The results show that the effects of inhomogeneous anisotropic conductivity of WM on the scalp EEG are significant.

Key words inhomogeneous anisotropic conductivity, finite element method, conductivity ratio approximation, statistical conductivity approximation.

Introduction

The electrical activity in the brain is caused by some chemical actions within neurons which produce potential differences[1]. The measurement of these potential differences between various locations at the surface of the scalp is called EEG[1,2]. The estimation of the potentials at scalp with known source configuration is termed as EEG forward problem[2-4]. The forward problem is a part of source localization or inverse problem[2-4], which is used for diagnosing neurological disorders (such as epilepsy), analysis of the depth of anaesthesia, origin of evoked potentials and other brain research functions[5]. In order to solve the forward problem, human head is modelled as a volume conductor. The accuracy of volume conductor depends on head geometry and conductivity. Since the volume conductor model represents the conductivity distribution in the head, therefore, it needs accurate conductivity for each head element. If conductivity is inaccurately assigned, it makes a significant effect on source localization[5]. It is known that human head is composed of different tissue layers which have different conductivities[5-7]. According to the physiological structure, there is further discrimination to each tissue layer. Scalp layer is also divided into the fat and muscle layers. Skull consists of a soft bone layer (spongiosa) enclosed by two hard bone layers (compacta). Since the spongiosa has a much higher conductivity than compacta, the skull shows an anisotropic conductivity with a ratio of 1 to 10 to the skull surface[6,8,9]. Skull resistivity varies between 1360 Ωcm and 21400 Ωcm, with a mean of 7560 Ωcm and a standard deviation of 4230 Ωcm. It is also known that the brain white matter has an anisotropic conductivity with a ratio of about 1 to 10 [5,6,10,11]. WM has the mean resistivity 700 Ωcm with 350 Ωcm and 1050 Ωcm values for lower and upper bounds, respectively, having the variation of ±50%[23]. Therefore, the skull and WM exhibit the inhomogeneous and anisotropy properties. Due to the complication of tissue type, fiber direction, the irregular structure and segmentation difficulties, there are some constraints: Volume constraint[6,7,14] and Wang's constraint[6,7,15] to implement inhomogeneous anisotropy model. Volume constraint restricts the geometric mean and the volume of the conductivity tensor as constant. And Wang's constraint restricts the direction of longitudinal and transverse conductivities as constant. Wolters *et al*[6,7] generated WM anisotropic conductivities for both constraints using different conductivity ratios to show the effect of anisotropy on head modelling. Li *et al*[11] generated inhomogeneous anisotropic conductivity for Volume constrained WM elements using the fractional anisotropy

Corresponding author: Rezaul Bashar, Department of Mathematics and Computing, Centre for Systems Biology, University of Southern Queensland, Toowoomba, QLD 4350, Australia, Tel: + 61 7 4631 1158, Fax: + 61 7 4631 5550
Email: bashar@usq.edu.au
Received: 12 February 2008; Accepted: 2 June 2008

(FA) obtained from diffusion tensor magnetic resonance images (DT-MRIs)[16]. They found that WM anisotropy and inhomogeneity would affect the scalp EEG. Gullmar *et al*[12,13] also generated anisotropic conductivities for Volume constrained WM and simulated on rabbit head model. They mentioned that the anisotropy of WM conductivity affect the EEG forward and inverse computations. Most recently, Hallez *et al*[14] implemented anisotropic conductivity for Volume constrained WM to analyse the source localization error. They showed that source localization is affected by WM anisotropy. However, to the best of our knowledge, no research has been done on Wang's constraint in WM inhomogeneous anisotropic conductivity.

The purpose of this study is to investigate the effects of WM inhomogeneous anisotropic conductivity on EEG forward computation. In particular, we focus our attention on two related problems: Are there any effects of inhomogeneous anisotropic conductivity on forward computing? Does the Volume or Wang's constraint affect on EEG? In this paper**,** we introduce new techniques, conductivity ratio approximation (CRA) technique and statistical conductivity approximation (SCA) technique to generate inhomogeneous anisotropic conductivity for constrained WM. We consider the inhomogeneity into two categories: (i) the discrepancy ratio of the longitudinal over transverse directional eigen values (Study I); (ii) the discrepancy of two transverse eigen values (Study II). We use a spherical model to simulate the head volume conductor with different inhomogeneous anisotropic conductivities for WM elements using finite element method (FEM). A current dipole inside the gray matter (GM) is used to simulate the electrical activity. The effects of WM inhomogeneous anisotropy on the scalp EEG are assessed by comparing the scalp potentials generated by inhomogeneous anisotropic with homogeneous isotropic and anisotropic WM conductivity models, separately.

This paper is structured as the following. The Introduction section provides a brief literature review. The Problem formulation section defines the head modelling and forward problem. The Homogeneous anisotropic conductivity section describes the Volume and Wang's constraints. Inhomogeneous anisotropic conductivity section defines CRA and SCA techniques. The Forward computation section presents the forward simulation and error measurements. The Simulation and experiment section illustrates the experimental setup. The Result analysis section describes the experimental result found in this research. And finally, Conclusion section summarizes our research findings.

Problem formulation

Anatomically, human head is made up of scalp, skull and brain layers. The brain layer, surrounded by cerebrospinal fluid (CSF), is divided into gray matter (GM) and white matter (WM). Human head is modelled either spherically[2,5,9] or realistically[6-8]. In spherical model, most researchers prefer three or four layered model. However, Hallez *et al*[5] proposed a five-layered spherical head model with scalp, skull, cortical, WM and thalamus shell. Wolters *et al*[31] also constructed a realistic head model with scalp, skull, CSF, GM and WM. Based on these anatomical concepts and literature[5-9,30-31], we consider a five-layered spherical head of scalp, skull, CSF, GM, and WM layers with radii of 8.8cm, 8.5cm, 8.1cm, 7.9cm and 6.5cm, respectively. We segment this five-layered sphere and perform mesh generation which produces tetrahedral elements for FEM. Based on literature[2,6,] we set the homogeneous isotropic conductivities as σ = 0.33 S/m (skin), σ = 0.0042 S/m (skull), σ = 1.0 S/m (CSF), σ = 0.33 S/m (GM), and σ = 0.14 S/m (WM), respectively. Though both the skull and the WM layers are inhomogeneous and anisotropic, in this study, we consider only WM layer as inhomogeneous and anisotropic while we treat other layers as homogeneous and isotropic. To apply FEM, we assign anisotropic conductivity tensor to each element of the WM layer. We assume that the conductivity tensors share the same eigen vectors with the effective diffusion tensors measured by DT-MRI[6,7,12,13,21]. Then, we consider the conductivity tensor for a WM finite element as[6,7,12,13]

$$\sigma = \mathbf{S}\begin{pmatrix} \sigma_{long} & 0 & 0 \\ 0 & \sigma_{trans} & 0 \\ 0 & 0 & \sigma_{trans} \end{pmatrix}\mathbf{S}^{-1} \quad (1)$$

where **S** is orthogonal matrix of unit length eigenvectors of the measured diffusion tensor at the barycentre of the WM finite element, σ_{long} is the parallel (longitudinal) eigen values and σ_{trans} is the perpendicular (transverse) eigen values where $\sigma_{long} \geq \sigma_{trans}$.

Mathematically, the forward problem is described by Poisson's equation for electrical conduction in a human head as shown below[2,3,6]

$$\nabla \bullet \sigma(\nabla\varphi) = -I_{sv} \quad \text{in } \Omega \quad (2)$$

where σ is a conductivity tensor and I_{sv} is internal current source per unit volume (Ω) due to current dipoles placed within the brain. The unknown φ is the electric potential created in the head by the distribution of current from the dipole sources. Then the forward problem is solved by applying the Newman boundary condition as [18,19]

$$\sigma(\nabla\varphi) \bullet \mathbf{n} = 0 \quad \text{on } \Gamma \quad (3)$$

where **n** is the unit surface normal and Γ is the surface.

Homogeneous anisotropic conductivity

In this study, we, firstly, use isotropic conductivity and simulate the anisotropic conductivity ratios according to Wolters *et al*[6,7]. Then, we calculate the longitudinal and transverse eigen values using either Volume or Wang's constraint.

Volume constraint

DT-MRI doesn't measure conductivity tensor directly but rather infers from the diffusion tensors which describes

the movement of both water molecules and electrically charged particles (ions)[12]. To implement conductivity tensor we assume that the same structural features that result in anisotropic mobility of water molecules also result in anisotropic conductivity. This assumption can be expressed as the eigen vectors of the conductivity tensor, similar as those from water diffusion tensor[21]. However, there are some problems for the conductivity tensor reconstruction process as addressed by Zhao *et al*[22]. One of them is the volume caused by low spatial resolution[22]. Volume varies due to several factors, such as age, diseases, environmental factors, and personal constitutions[7,23]. To overcome volume obstacle, Wolters[6] proposed Volume constraint, which restricts the geometric mean and the volume of the conductivity tensor as constants. The Volume constraint is defined as [6,7,12]

$$\frac{4}{3}\pi\sigma_{long}\left(\sigma_{trans}\right)^2 = \frac{4}{3}\pi\sigma_{iso}^3 \tag{4}$$

where σ_{iso} is isotropic conductivity.

Wang's constraint

Another problem for the conductivity tensor reconstruction process is the movement of water molecules (direction). Water molecules usually move towards the high conductivity direction. In white matter, the diffusion of water molecules perpendicular to fiber direction is slower than parallel[21,22]. To stay constant for these molecules, Wang *et al*[15] proposed a constraint method. Wang's constraint is defined as the product of longitudinal and transverse conductivities is constant and is equal to the square of the isotropic conductivity. It is represented as [6,7,15]

$$\sigma_{long}.\sigma_{trans} = \sigma_{iso}^2 \tag{5}$$

Inhomogeneous anisotropic conductivity for Study I

To implement inhomogeneous anisotropy, Li *et al*[11] proposed threshold controlled fractional anisotropy (FA) using step and linear functions. They used two thresholds and three slopes. However, there is no reliable algorithm to construct inhomogeneous anisotropic conductivity[11,12]. In this study we propose conductivity ratio approximation (CRA) and statistical conductivity approximation (SCA) techniques.

Conductivity ratio approximation

From the literature[6,7,12,13] it is understood that the anisotropic conductivity ratio varies from 1 to 10, which can be expressed as

$$\sigma_{long} : \sigma_{trans} = \xi : 1 \text{ where } \xi = 1 \text{ to } 10 \tag{6}$$

Based on these concepts, we apply CRA to construct the inhomogeneous anisotropic model. Firstly, we generate a vector **r** with all possible conductivity ratios from 1 to 10. Secondly, we select the conductivity ratio ξ_{lt} using random selection, where $\xi_{lt} \in$ **r** for each element**.** Based on this conductivity ratio ξ_{lt}, we determine the longitudinal and inhomogeneous conductivities by means of eq (4). However, we only select those whose values satisfy $\sigma_{long} \geq \sigma_{trans}$. For example, if ξ_{lt} is 2, then the longitudinal and transverse conductivities are 0.222 and 0.111, respectively. Finally, using the similar procedure, we determine the longitudinal and transverse inhomogeneous anisotropic conductivity for Wang's constraint applying eq(5) in place of eq(4).

Statistical conductivity approximation

Shimony *et al*[24] measured diffusion anisotropy in 12 regions of interest in human white and gray matters. Gullmar *et al*[13] showed that Rayleigh distribution fits the mean and variance of their experimental results, which produces prolate shape. Therefore, we assume that Rayleigh distribution can generate random numbers that fits the inhomogeneous anisotropic conductivities for WM. The probability density function (pdf) of Rayleigh distribution is defined as[25]:

$$f(x,\sigma) = \frac{x}{\sigma^2} e^{\left(\frac{-x^2}{2\sigma^2}\right)}; \quad \mathbf{x} \in [0,\infty) \tag{7}$$

where ***x*** is a vector of random variables and σ is the only parameter which equals to the mode of Rayleigh distribution.

The mean, variance and cumulative density function (cdf) of Rayleigh distribution are as

$$mean = \sigma\sqrt{\frac{\pi}{2}} \tag{8}$$

$$\text{var} = \frac{4-\pi}{2}\sigma^2 \tag{9}$$

$$cdf = 1 - e^{\frac{-x^2}{2\sigma^2}} \tag{10}$$

We select the inverse transform method for random number generation[25,26]. The following algorithm generates the random numbers which meet Rayleigh distribution. Firstly, we determine **X** = random number generated from uniform distribution. We set the mean conductivities according to literature[2,6,12]. Then we determine σ based on eq(8). Finally, we determine the random numbers according to Rayleigh distribution by applying the cdf defined in eq(10). We treat these random numbers as longitudinal inhomogeneous conductivities. And based on these conductivities we determine the transverse inhomogeneous conductivities by using Volume and Wang's constraints where $\sigma_{long} \geq \sigma_{trans}$, repectively.

Inhomogeneous anisotropic conductivity for Study II

Tissue anisotropy means that the electrical conductivity of this tissue is direction dependent as shown in figure 1, where one longitudinal and two transversal directions are shown[5]. Some literature[6-7,12-13] assume that two transverse conductivity eigen values presented in eq(1) are identical.

Based on this assumption we calculate the inhomogeneous anisotropy conductivity in Study I. However, in other literature[11,14], it is found that these two transverse conductivity eigen values are not the same every where in WM due to the fiber-crossing. These eigen values produce a ratio from 1 to 10[11].

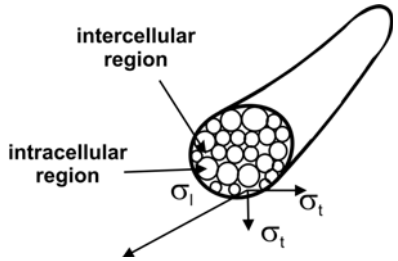

Figure 1. *Anisotropic conductivities of white matter[5] σ_l represents longitudinal and σ_t represents represents transversal conductivity.*

In Study II, we consider the ratio between these two transverse conductivities. We consider the same ratio (ξ_{lt}) produced in Study I by CRA for these transverse conductivity ratios (ξ_{tt}) such that $\forall_x\left(\xi_{tt}(x)\rightarrow(\xi_{lt})\right)$, however, we select ξ_{tt} in random order. We also generate the inhomogeneous longitudinal and transverse conductivities by means of both constraints, separately. The Volume constraint stated in eq(4) can be redefined as[11,14]

$$\frac{4}{3}\pi\sigma_{long}\sigma_{trans1}\sigma_{trans2}=\frac{4}{3}\pi\sigma_{iso}^{3} \tag{11}$$

σ_{trans1} and σ_{trans2} represent two transverse conductivities where $\sigma_{long}:\sigma_{trans1}=\xi_{lt}$ and $\sigma_{tran1}:\sigma_{trans2}=\xi_{tt}$. For example, if ξ_{lt} is 3 and ξ_{tt} is 2, then σ_{long}, σ_{trans1}, σ_{trans2} values are 0.3699, 0.1223 and 0.0612, respectively. In this case, Li *et al*[11] used $\sigma_{long}:\sigma_{trans1}=\xi_{lt}=\sigma_{long}:\sigma_{trans2}$ but we don't consider it as an inhomogeneous. Because σ_{trans1} always shows WM isotropic conductivity (σ = 0.14). For example, if ξ_{lt} = 3, then it produces the values of σ_{long} = 0.42, σ_{trans1} = 0.14, and σ_{trans2} = 0.046667. Again if ξ_{lt} = 5, it produces the values of σ_{long} = 0.7, σ_{trans1} = 0.14, and σ_{trans2} = 0.028. To avoid this situation we use $\sigma_{long}:\sigma_{trans1}=\xi_{lt}$ and $\sigma_{tran1}:\sigma_{trans2}=\xi_{tt}$. For Wang's constraint we consider eq(5) while σ_{trans} represents average of σ_{tran1} and σ_{tran2}. For SCA, we determine the longitudinal conductivities according to Study I and then we apply eq(11) for Volume constraint and eq(5) for Wang's constraint in the similar manner as CRA.

Forward computation

The EEG forward computation is performed by assigning conductivity to the individual elements putting a current source in the volume conductor (here, head is used as volume conductor). The Poisson equation in eq(2) and eq(3) are solved by means of FEM. For the modelling of the current source, we use 'single dipole', which has been introduced by Yan *et al*[20]. We use a standard variation procedure to transform the Poisson equation from the quasi-static Maxwell's equations into an algebraic system of linear equations. We solve the linear equations by preconditioned conjugate gradient method[6] using Cholesky factorization preconditioning[29] with a drop tolerance of $1e^{-4}$. We calculate the electric potentials produced by a single dipole for both radial and tangential sources using 64 electrodes positioned at different places on a head surface[27]. The forward computed data obtained from the homogeneous isotropic, homogeneous anisotropic and inhomogeneous anisotropic models are analysed by calculating relative difference measure (RDM) for the topology errors (minimum error: RDM=0) and magnitude difference (MAG) values (minimum error: MAG=1) of the electric potentials. Homogeneous isotropic model is obtained by assigning homogeneous isotropic conductivities. The homogeneous anisotropic model[11] is obtained by setting the maximum conductivity ratio. The inhomogeneous anisotropic model is obtained by assigning inhomogeneous anisotropic conductivity. The RDM and MAG values are calculated as follows[12,28]:

$$RDM=\sqrt{\sum_{i=1}^{n}\left(\frac{ref_i}{\sqrt{\sum_{i=1}^{n}ref_i^{\,2}}}-\frac{meas_i}{\sqrt{\sum_{i=1}^{m}meas_i^{2}}}\right)^{2}} \tag{12}$$

$$MAG=\sqrt{\frac{\sum_{i=1}^{m}meas_i^{2}}{\sum_{i=1}^{m}ref_i^{\,2}}} \tag{13}$$

where the values obtained from the homogeneous isotropic or homogeneous anisotropic model are interpreted as reference (ref) and the values obtained from the inhomogeneous anisotropic model are used as measurement (meas). The index *i* represents the numbers of electrodes.

Simulation and experiment

Firstly, we implement a five-layered concentric spherical head model[5] with the radii shown in row 2 in table 1 using Matlab[29]. Secondly, We segment the head model into surfaces, perform tessellation for mesh generation, and then apply a constrained Delaunay tessellation technique[29] using Tetgen® package provided by Baillet *et al*[27]. The mesh generation produces 315K tetrahedral elements from 54K nodes shown in table 1 (last row). We use these tetrahedral elements for FEM modelling. For homogeneous isotropic case, we assign the mean WM conductivity studied from several samples of that tissue type to each element (row 3 in table 1) and we also assign anisotropic WM conductivity using $\sigma_{long}:\sigma_{trans}=10$ for homogeneous anisotropic head model. However, we assign the

Table 1. *Head model parameters.*

	Scalp	Skull	CSF	GM	WM
Radii (cm)	8.8	8.5	8.1	7.9	6.5
Means (S/m)	0.33	0.0042	1.0	0.33	0.14
Elements	52519	67403	278846	66665	50489

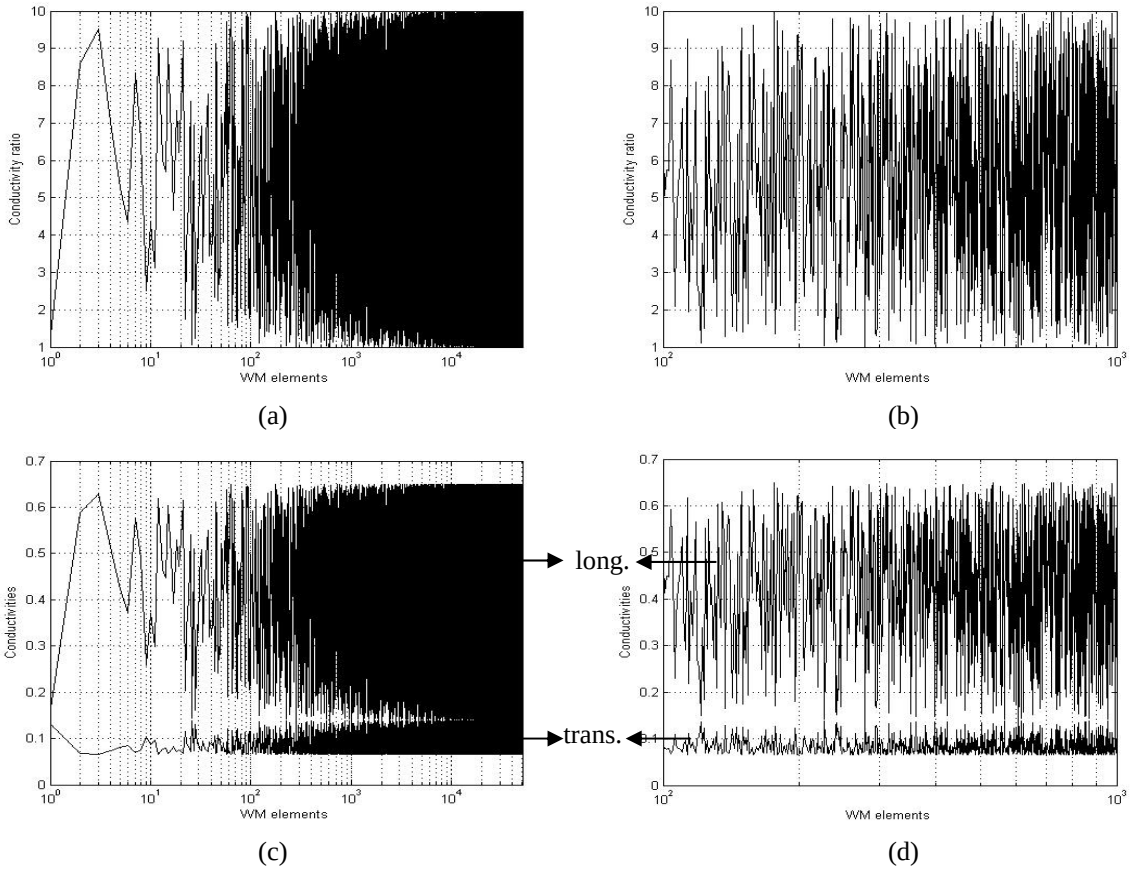

Figure 2. *(a) Value of conductivity ratio (ξ_{lt}) between longitudinal and transverse conductivity for each WM element generated by CRA, (b) clear view of (a) from 10^2 to 10^3 WM elements, (c) longitudinal (long.) and transverse (trans.) conductivity values for each WM elements based on ξ_{lt} of (a) using Volume constraint, and (d) clear view of (c) from 10^2 to 10^3 WM elements.*

conductivities produced by CRA or SCA (shown in figures 2(c) or 3(c)) to individual WM elements for the inhomogeneous anisotropic purpose. We also implement CRA and SCA techniques in Matlab. For both homogeneous isotropic and inhomogeneous anisotropic cases, we assign the homogeneous isotropic conductivity to other head layers. After assigning conductivities, we perform forward computation using the adopted FEM tool provided by Baillet *et al*[27]. We place a fixed dipole at 2mm below the cortex surface inside the GM[32] with the azimuth and elevation orientations $\pi/4$ and $\pi/5$, respectively. We choose the unit magnitude of the dipole and consider XY plane only. We measure the EEG using 64 electrodes. Finally, we apply RDM and MAG techniques to analyse the results. We implement those computations using an Intel® dual core 2.0 Ghz processor. It takes approximately 3 hours to carry out each computation.

To investigate the influence of inhomogeneous anisotropic WM conductivity, two types of experiments are carried out. Each Study uses the same head model except their conductivities.

The conductivity ratio between longitudinal and transverse for each element is generated using the CRA. Based on this ratio, we determine the longitudinal and transverse conductivities by applying either Volume or Wang's constraint for WM tissue layer. In the case of homogeneous anisotropic model, ξ_{lt} is constant. For example, Wolters *et al*[6,7] and Gullmer *et al*[13] used 1,2,5 or 10 for the value of ξ_{lt} . However, for inhomogeneous anisotropic case, ξ_{lt} can be 1 to 10. CRA generates different values for ξ_{lt} as shown in figure 2(a). Figure 2(c) shows the longitudinal and transverse conductivities for Volume constraint generated by means of the values of ξ_{lt} shown in figure 2(a). In the similar way, we generate

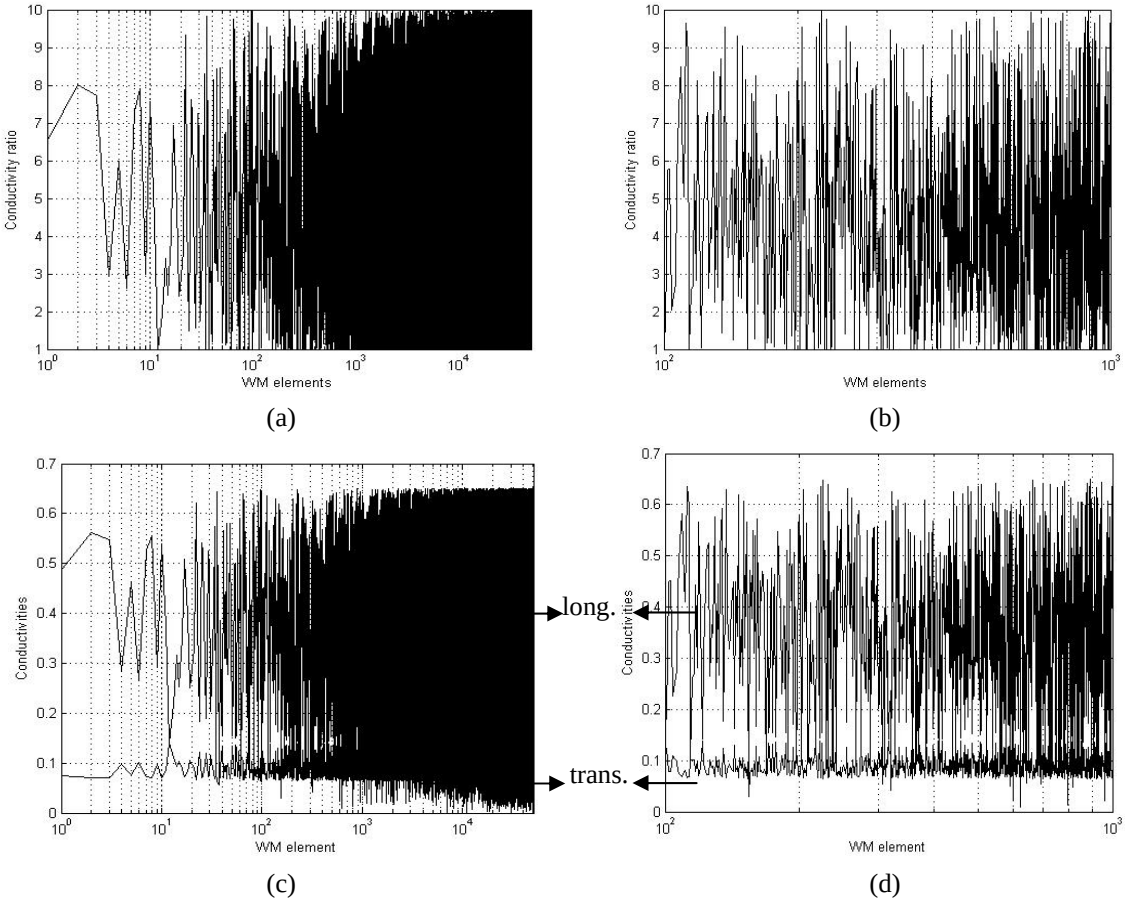

Figure 3. *(a) Value of ξ_{lt} (conductivity ratio) between longitudinal and transverse conductivity for each WM element generated by SCA, (b) clear view of (a) from 10^2 to 10^3 WM elements, (c) longitudinal and transverse conductivity values for each WM elements based on ξ_{lt} of (a) using Volume constraint, and (d) clear view of (c) from 10^2 to 10^3 WM elements.*

Table 2. *RDM and MAG values between homogeneous isotropic (homo_iso) and inhomogeneous anisotropic (inho_aniso) models, and homogeneous anisotropic(homo_aniso) and inho_aniso models using conductivity ratio approximation for Study I calculated by either Volume or Wang's constrained conductivities.*

	Conductivity	homo iso vs inho aniso		homo aniso vs inho aniso	
		RDM	MAG	RDM	MAG
Volume constraint	longitudinal	27.60%	1.4384	6.47%	0.9023
	transverse	28.21%	0.9104	42.06%	0.9518
Wang's constraint	longitudinal	19.16%	1.2637	6.11%	0.79
	transverse	32.90%	0.8923	45.15%	0.9329

longitudinal and transverse conductivities for Wang's constraint.

The SCA determines the random numbers using Rayleigh distribution, which we consider as longitudinal conductivities. Later on, we generate transverse conductivities according to either Volume or Wang's constraint. Similar as figure 2, figure 3 shows the conductivity ratio (figure 3(a)) and conductivities for Volume constrained WM (figure 3(c)). Comparing figure 2 and figure 3, we see that CRA produces higher conductivity ratios than SCA.

Result analysis

To analysis our research findings we compare inhomogeneous anisotropic results with both of homogeneous isotropic (homo_iso vs inho_aniso) and homogeneous anisotropic (homo_aniso vs inho_aniso) results for each case.

Study I

Table 2 presents the RDM and MAG values produced by the CRA technique. For all the cases, RDM and MAG

Table 3. *RDM and MAG values between homogeneous isotropic (homo_iso) and inhomogeneous anisotropic (inho_aniso) models, and homogeneous anisotropic (homo_aniso) and inho_aniso models using statistical conductivity approximation for Study I computed by either Volume or Wang's constraint assuming the identical longitudinal conductivities.*

	Conductivity	homo_iso vs inho_aniso		homo_aniso vs inho_aniso	
		RDM	MAG	RDM	MAG
Volume constraint	longitudinal	19.91%	1.3056	5.09%	0.8235
	transverse	24.55%	0.9458	39.38%	0.9888
Wang's constraint	transverse	18.61%	0.8471	36.44%	0.8856

Table 4. *RDM and MAG values between homogeneous isotropic (homo_iso) and inhomogeneous anisotropic (inho_aniso) models, and homogeneous anisotropic(homo_aniso) and inho_aniso models using conductivity ratio approximation for Study II calculated by either Volume or Wang's constrained conductivities. Transverse1 and transverse2 represent two transverse directional conductivities shown in figure 1.*

	Conductivity	homo_iso vs inho_aniso		homo_aniso vs inho_aniso	
		RDM	MAG	RDM	MAG
Volume constraint	longitudinal	23.56%	1.4505	1.278%	0.9148
	transverse1	4.99%	0.9635	36.12%	1.00
	transverse2	35.52%	0.7852	46.12%	0.8209
Wang's constraint	longitudinal	19.36%	1.2185	5.9%	0.7686
	transverse1	30.88%	0.9235	43.89%	0.9656
	transverse2	21.85%	0.7373	37.27%	0.77089

values are far from the ideal values, 0 and 1, respectively. This indicates a strong affect of WM inhomogeneous anisotropy on EEG. While we implement inhomogeneous anisotropy, different conductivities rather than homogeneous isotropy are assigned. Therefore, electrical potentials vary from the reference model. Volume constrained σ_{long} and Wang's constrained σ_{trans} are more affected by inhomogeneous anisotropy. From eq(4) and eq(5), we find that the Volume constrained σ_{long} has higher values and Wang's constrained σ_{trans} has lower values. These two conductivity values are far away from the homogeneous isotropic conductivity (0.14). For instance, when ξ_{lt} = 10, the value of σ_{long} and σ_{trans} are 0.65 and 0.044 for Volume and Wang's constraints, respectively. In comparison with homogeneous anisotropic model, inhomogeneous anisotropic models produce less MAG error. In our experiment, we consider ξ_{lt} = 10 for homogeneous anisotropic model. As our inhomogeneous anisotropic model is generated by different conductivity ratios (1 to 10) defined in eq(6) and shown in figure 2(a), therefore, it produces big magnitudes than the reference model. As a result, it becomes closer to homogeneous anisotropic model. Here, the MAG is 1.58 between reference and homogeneous anisotropic models. The longitudinal conductivities for both constraints are more affected by homogeneous isotropy than homogeneous anisotropy (comparing columns 5 and 6 with columns 3 and 4 for longitudinal conductivities). However, transverse conductivities are more affected by homogeneous anisotropy than homogeneous isotropy as shown in row 3 and row 5 in table 2.

Table 3 shows the results of the topology and magnification errors where the inhomogeneity is determined using the SCA technique. Tables 2 and 3 show the similar results, namely, the WM inhomogeneous anisotropy has a strong effect on EEG. Wang's constrained transverse conductivities produce higher MAG and lower RDM error than that of Volume constraint. In this case, we calculate transverse conductivities for both constraints using the same longitudinal conductivities. For example, if the value of σ_{long} = 0.65, then σ_{trans} = 0.065 for Volume constraint and σ_{trans} = 0.0302 for Wang's constraint (applying eq(4) and eq(5). In a way, applying Volume constrained transverse conductivities; we obtain the magnification values (0.9888) close to homogeneous anisotropic model. Though the RDM values produced by Wang's constrained transverse conductivities are comparatively lower than that of Volume constraint, but it produces higher MAG errors (3rd and 4th rows in table 3). Comparing CRA technique with SCA**,** it is found that CRA produced conductivities generate more topology and magnification errors than those of SCA.

Study II

Table 4 presents the RDM and MAG values produced by CRA technique based on Study II for both constraints. These experiments also demonstrate that WM inhomogeneous anisotropy has a strong effect on EEG. According to eq(11), the value of Volume constrained σ_{trans1} is very close to isotropic conductivity (0.14). For

Table 5. *RDM and MAG values between homogeneous isotropic (homo_iso) and inhomogeneous anisotropic (inho_aniso) models, and homogeneous anisotropic (homo_aniso) and inho_aniso models using statistical conductivity approximation for Study II computed by Volume or Wang's constraint assuming the identical longitudinal conductivities. Transverse1 and transverse2 represent two transverse directional conductivities shown in figure 1.*

	Conductivity	homo_iso Vs inho_aniso		homo_aniso Vs inho_aniso	
		RDM	MAG	RDM	MAG
Volume constraint	longitudinal	19.98%	1.2327	5.34%	0.7775
	transverse1	17.61%	0.9878	36.72%	1.0327
	transverse2	40.34%	0.8301	50.06%	0.8679
Wang's constraint	transverse1	18.80%	0.8628	36.31%	0.9021
	transverse2	41.56%	0.8432	48.37%	0.8314

example, if ξ_{lt} is 5 and ξ_{tt} is 3, then σ_{long}, σ_{tran1}, σ_{tran2} values are 0.590403, 0.118081, and 0.039360, respectively, for Volume constraint. As a result, σ_{trans1} produces less RDM and MAG errors than others. Similarly, Wang's constrained values are 0.313050, 0.093915, and 0.031305, respectively. Volume constrained σ_{long} generates more RDM (23.56%) and MAG (1.4505) errors than Wang's constrained σ_{long} (RDM = 19.36% and MAG = 1.2185). Volume constrained σ_{trans1} and σ_{trans2} generate less MAG errors than those of Wang's constraint. Like table 2, we observe here, the longitudinal conductivities for both constraints are more affected by homogeneous isotropy than homogeneous anisotropy (comparing columns 5 and 6 with columns 3 and 4 for longitudinal conductivities in table 4). However, transverse conductivities are more affected by homogeneous anisotropy than homogeneous isotropy (rows 3,4, 5 and 6 in table 4).

Table 5 shows the RDM and MAG values where the inhomogeneity is obtained from SCA produced conductivity ratio (ξ_{tt}). The similar results presented in tables 2-4 are also observed in table 5. Comparing table 5 with table 4, we also found that CRA based conductivities are more affected than SCA based conductivities.

In this experiment, RDM and MAG errors between the reference model and homogeneous anisotropic model are 23.85% and 1.5854, respectively, for longitudinal conductivity. According to the conductivity generation, inhomogeneous anisotropic models are produced by less conductivity ratios than homogeneous anisotropic model. As a result, all of the RDM and MAG errors in this experiment are lower than those values. Similarly, the reference model and homogeneous anisotropic model generated by transverse conductivity produce 35.11% RDM and 0.9565 MAG errors. Most of our RDM and MAG errors are close to above mentioned values except σ_{trans2}. As these conductivity values are generated by random numbers, in some cases it produces more errors than above mentioned values, for example σ_{trans2}. Therefore, by using inhomogeneous anisotropic model in place of homogeneous anisotropic model we are able to reduce RDM and MAG errors.

Conclusion

In this study, we apply the conductivity ratio approximation and statistical conductivity approximation techniques to assign the longitudinal versus transverse WM conductivity ratio for inhomogeneous anisotropic head model. The preliminary results show that EEG is affected by the WM inhomogeneous anisotropic conductivity in the both models generated by using the Volume constraint and Wang's constraint. On the one hand, the model generated by using Volume constraint is more influenced by its longitudinal conductivity inhomogeneity. On the other hand, the model generated using Wang's constraint is more influenced by its transverse conductivity inhomogeneity.

In this study, we use five-layered spherical head model; however, we consider the similar approaches for realistic head model by assuming the random anisotropy in lieu of DT-MRI data. Therefore, more similar studies of inhomogeneous and anisotropy tissue conductivity will be thoroughly investigated in the future using realistic head model from DT-MRI. Although this study does not quantify the absolute errors, we conclude that incorporating the WM inhomogeneous anisotropy effects on the EEG forward solution by up to 50% in RDMs and 0.7 to 1.45 in MAGs when compared with homogeneous isotropy and anisotropy models.

Acknowledgement

This project is supported by ARC Discovery Program: DP0665216, and University of Southern Queensland Research Infrastructure Program 2006 and 2007.

References

1. Kervinen, M., Vauhkonen, M. and Karjalainen, P. A., *New Continuous Current density Model for EEG*, Biosignal Analysis and Medical Imaging Group, University of Kuopio, Finland (http://bsamig.uku.fi/pdf/CDmanuscript.pdf).
2. Wen, P., *Human Head Modelling and Computation for the EEG Forward Problem*, PhD dissertation, The Flinders University of South Australia, Australia, 2000.

3. Muravchik, C. and Nehorai, A., *EEG/MEG Error Bounds for a Static Dipole Source with a Realistic Head Model*, IEEE Transactions on Biomedical Engineering, 49(3), 470-483, 2001.
4. Xie, Y., Yuan, J., Ma, X. and Guan, X., *Calculating of EEG problems with Anisotropic Conducting Media by the Finite Volume Method*, IEEE Transactions on Magnetics, 37(5), 3749-3752, 2001.
5. Hallez, H., Hese, V., Vanrumste, B., Boon, P., Asseler, Y. D., Lemahieu, I. and Walle, R. Van de, *Dipole Localization Errors due to not Incorporating Layers with Anisotropic Conductivities: Simulation Study in a Spherical Head Model*, International Journal of Bioelectromagnetism (IJBEM), 7(1), 134-137, 2005.
6. Wolters, C. H., *Influence of Tissue Conductivity Inhomogeneity and Anisotropy on EEG/MEG based Source Localization in the Human Brain*, PhD dissertation, University of Leipzig, France, 2003.
7. Wolters, C. H., Anwander, A., Tricoche, X., Weinstein, D., Koch, M. A. and MacLeod, R. S., *Influence of tissue conductivity anisotropy on EEG/MEG field and return current computation in a realistic head model: A simulation and visualization study using high-resolution finite element modelling*, Journal of NeuroImage, Elsevier, 30, 813-826, 2006.
8. Marin, G., Guerin, C., Baillet, S., Garnero, L. and Meunier, G., *Influence of Skull Anisotropy for the Forward and Inverse Problem in EEG: Simulation Studies using FEM on Realistic Head Models*, Journal of Brain Mappings, 6, 250-269, 1998.
9. Nicolas, C., Xavier, F., Bernard, D., Bernard, R., Jean, P. M. and Pierre, C., *Effects of Skull Thickness, Anisotropy, and Inhomogeneity on Forward EEG/ERP Computations Using Spherical Three-Dimensional Resistor Mesh Model*, Journal of Human Brain Mapping, 21, 86-97, 2004.
10. Bruno, P. , Hyttinen J., Inchingolo, P. , Magrofuoco, A. , Mininel, S. and Vatta, F. , *A FDM anisotropic formulation for EEG simulation*, IEEE EMBS Annual International Conference, New York, USA, 1121-1125, 2006.
11. Li, L., Wang, K., Zhu, S., Mueller, K., Lim, K., Liu, Z. and He, B., *A Study of White Matter Anisotropic conductivity on EEG Forward Solutions*, Proceedings of Noninvasive Functional Source Imaging of the Brain and Heart and the International Conference on Functional Biomedical Imaging (NFSI & ICFBI-IEEE explorer), 130-132, 2007.
12. Gullmar, D., Haueisen, J., Wiselt, M., Giebler, F., Flemming, L., Anwander, A. Thomas, R. K., Wolters, C. H., Dumpelmann, M., David, S. T. and Jurgen, R. R., *Influence of Anisotropic Conductivity on EEG source Reconstruction: Investigations in a Rabbit Model*, IEEE Transactions on Biomedical Engineering, 53(9), 1841-1850, 2006.
13. Gullmar, D., Jurgen, R. R. and Haueisen, J., *Influence of anisotropic conductivity on EEG forward and inverse solution*, Proceedings of Noninvasive Functional Source Imaging of the Brain and Heart and the International Conference on Functional Biomedical Imaging (NFSI & ICFBI-IEEE explorer), 124-126, 2007.
14. Hallez, H., Vanrumste, B., Hese, P. V., Delputte, S., and Lemahieu, I., *Dipole estimation errors due to differences in modelling anisotropic conductivities in realistic head models for EEG source analysis*, Journal of Physics in Medicine and Biology, IOP Publishing, 53, 1877-1894, 2008.
15. Wang, Y., David, R. H. and Kim, Y., *An Investigation of the Importance of Myocardial Anisotropy in Finite-Element Modeling of the Heart:Methodology and Application to the Estimation of Defibrillation Efficacy*, IEEE Transactions on Biomedical Engineering, 48(12), 1377-1389, 2001.
16. Kim, S., Kim, T. S., Zhou, Y. and Singh, M., *Influence of Conductivity Tensors in the Finite Element Model of the Head on the Forward Solution of EEG*, IEEE conference on Nuclear Science Symposium Conference Record, 1892-1896, 2001.
17. Wen, P. and Li, Y., *EEG human head modelling based on heterogeneous tissue conductivity*, Australasian Physical & Engineering Sciences in Medicine, 29(3), 235-240, 2006.
18. Marc, A. C., John, L. L. and Solomon, R. E., *A Three-Dimensional Finite Element Model of Human Transthoracic Defibrillation: Paddle Placement and Size*, IEEE Transactions on Biomedical Engineering, 42(6), 572-578, 1995.
19. Klepfer, R. N., Johnson, C. R. and Robert, S. M., *The effects of Inhomogeneities and Anisotropies on Electrocardiographic Fields: A 3-D Finite –element Study*, IEEE Transactions on Biomedical Engineering, 44(8), 706-719, 1997.
20. Yan, Y., Nunez, P. L. and Hart, R. T., *Finite-element model of the human head: scalp potentials due to dipole sources*, Journal of Medical & Biological Engineering & Computing, 29, 475-481, 1991.
21. Basser, P., Mattiello, J. and LeBihan, D., *MR diffusion tensor spectroscopy and imaging*, Biophysical Journal, 66, 259-267, 1994.
22. Zhao, X., Wang, M., Gao, W. and Liu, H., *White Matter Fiber Tracking Method by Vector Interpolation with Diffusion Tensor Imaging Data in Human Brain*, Proceedings of the IEEE Engineering in Medicine and Biology 27 th Annual Conference, 5786-5789, 2005.
23. Hauseisen, J., Ramon, C., Eiselt, M., Brauer, H. and Nowak, H., *Influence of Tissue Resistivities on Neuromagnetic Fields and Electric Potentials studied with a Finite Element Model of the Head*, IEEE Transactions on Biomedical Engineering, 44(8), 727-735, 1997.
24. Shimony, J. S., McKinstry, R., Akbudak, E., Aronovitz, J. A., Snyder, A. Z., Lori, N. F., Cull, T. S. and Conturo, T.E., *Quantitative diffusion-tensor anisotropy brain MR imaging: Normative human data and anatomical analysis*, Radiology, 212, 770-784, 1999.
25. http://en.wikipedia.org/wiki/Rayleigh_distribution
26. Rodney, F. W., Gareth, J. J. and Kenneth, V. L., *Monte Carlo Simulation and Random Number Generation*, IEEE Journal on Selected Areas in Communications, 6(1), 58-66, 1988.
27. Baillet, S., Mosher, J. C. and Leahy R. M., *Electromagnetic Brain Imaging using Brainstorm*, IEEE International Symposium on Biomedical Engineering: Macro to Nano, 652-655, 2004.
28. Meijis, J.W., Weier, O. W., Peters, M. J. and Oosterom, A. van, *On the numerical accuracy of the boundary element method*, IEEE Transactions on Biomedical Engineering, 36(10), 1038-1049, 1989.
29. The Matlab, Mathworks limited.
30. http://en.wikipedia.org/wiki/Cerebral_cortex
31. Wolters, C. H., Anwander, A., Tricoche, X., Lew, B., and Johnson, C. R., *Influence of Local and Remote White Matter Conductivity Anisotropy for a Thalamic Source on EEG/MEG Field and Return Current Computation*, International Journal of Bioelectromagnetism (IJEM), 7(1), 203-206, 2005.
32. Noirhomme, Q., Kitney, R. I., and Macq, B., *Single-Trial EEG Source Reconstruction for Brain-Computer Interface*, IEEE Transactions on Biomedical Engineering, 55(5), 1592-1601, 2008.